






# The immune microenvironment in typical carcinoid lung tumour, a brief report of four cases

Branislava Stankovic<sup>1</sup>  | Henrik Aamodt<sup>1,2</sup> | Heidi Anine Korsmo Bjørhovde<sup>1</sup> | Elisabeth Müller<sup>1</sup> | Clara Hammarström<sup>3</sup> | Odd Terje Brustugun<sup>4,5</sup>  | Åslaug Helland<sup>5,6,7</sup>  | Inger Øynebråten<sup>1</sup>  | Alexandre Corthay<sup>1,8</sup> 

<sup>1</sup>Tumor Immunology Lab, Department of Pathology, Rikshospitalet, Oslo University Hospital and University of Oslo, Oslo, Norway

<sup>2</sup>Department of Cardiothoracic Surgery, Ullevål Hospital, Oslo University Hospital, Oslo, Norway

<sup>3</sup>Department of Pathology, Rikshospitalet, Oslo University Hospital, Oslo, Norway

<sup>4</sup>Section of Oncology, Drammen Hospital, Vestre Viken Hospital Trust, Drammen, Norway

<sup>5</sup>Department of Genetics, Institute for Cancer Research, The Norwegian Radium Hospital, Oslo University Hospital, Oslo, Norway

<sup>6</sup>Department of Oncology, The Norwegian Radium Hospital, Oslo University Hospital, Oslo, Norway

<sup>7</sup>Institute of Clinical Medicine, University of Oslo, Oslo, Norway

<sup>8</sup>Hybrid Technology Hub – Centre of Excellence, Institute of Basic Medical Sciences, University of Oslo, Oslo, Norway

## Correspondence

Branislava Stankovic and Alexandre Corthay, Tumor Immunology Lab, Department of Pathology, Rikshospitalet, Oslo University Hospital and University of Oslo, Oslo, Norway.  
Emails: brana.branislava.stankovic@gmail.com; alexandre.corthay@medisin.uio.no

## Funding information

This work was funded by the South-Eastern Norway Regional Health Authority (grant no. 2016111) and The Research Council of Norway (grant no. 262814).

## Abstract

Pulmonary typical carcinoid (TC) is a low-grade, rare lung cancer of neuroendocrine origin. Currently, there is very little information available about the immune cell composition in TC tumours. Here, we analysed by flow cytometry resected tumours from four never-smoker female patients with TC. Twelve distinct immune cell types were identified in TC tumours. The most abundant immune cells were CD8<sup>+</sup> T cells, CD4<sup>+</sup> T cells, B cells and macrophages, which represented 19.8%, 17.7%, 11.5% and 11% of all tumour-infiltrating CD45<sup>+</sup> leucocytes, respectively. Natural killer (NK) cells (8.8%) and neutrophils (3.9%) were also common. Three types of dendritic cells (DCs) were identified (plasmacytoid DCs, CD1c DCs, and CD141 DCs) which together constituted 1.4% of all immune cells in TC tumours. Small populations of basophils (1.2%), mast cells (0.8%) and eosinophils (0.6%) were also present. Notably, the percentage of leucocytes (of all living cells) was much lower in TC tumours compared to high-grade non-small cell lung cancer (NSCLC) tumours and also compared to non-cancerous lung tissue. We conclude that TC tumours are relatively non-inflammatory, although the immune landscape was found to be very complex.

This is an open access article under the terms of the Creative Commons Attribution License, which permits use, distribution and reproduction in any medium, provided the original work is properly cited.

© 2020 The Authors. Scandinavian Journal of Immunology published by John Wiley & Sons Ltd on behalf of The Scandinavian Foundation for Immunology

## 1 | INTRODUCTION

Pulmonary carcinoids are rare neuroendocrine tumours of the lungs with two subtypes: low-grade typical carcinoid (TC) and intermediate-grade atypical carcinoid.<sup>1-3</sup> Carcinoids represent 1%-2% of all primary lung cancers<sup>4,5</sup> and, contrary to most airways malignancies, are not linked to tobacco smoking. Instead, pulmonary carcinoid tumours have a low mutation rate and lack the characteristic smoking-related mutation signature.<sup>6</sup> The primary treatment option is surgery, which is curative for most patients. However, there is currently no efficient treatment for metastatic disease.<sup>4,7</sup>

The development of cancer immunotherapy in the past ten years has revolutionized the treatment of cancer. Monoclonal antibodies targeting immune checkpoint molecules, like PD-1, PD-L1 and CTLA-4, have become an established treatment option for multiple cancers, including non-small cell lung cancer (NSCLC).<sup>8-10</sup> The success of immunotherapy has led to an increased focus on the immune microenvironment of NSCLC which appears to be particularly complex.<sup>11-13</sup>

Contrary to high-grade NSCLC, the immune landscape of low-grade TC tumours is poorly described. In different reports, the percentage of TC tumours that were PD-L1-positive was generally low and varied from 0%-9%.<sup>14-17</sup> Vesterinen et al reported low numbers of PD-1-positive lymphocytes in some, but not all, TC tumours examined.<sup>17</sup> Kasajima et al<sup>15</sup> detected tumour-associated inflammation in only one out of 39 TC tumours investigated by immunohistochemistry. To the best of our knowledge, cytotoxic CD8<sup>+</sup> T cells represent the only immune cell type that has been identified with certainty in TC tumours so far.<sup>15-17</sup> Katsenelson et al found CD1a<sup>+</sup> and CD83<sup>+</sup> dendritic cells (DCs) in high-grade small cell lung cancer but none in bronchial carcinoid tumours.<sup>18</sup>

In this short report, we used multiparameter flow cytometry to analyse the immune cell content in resected tumours from four patients with TC. As many as twelve distinct immune cell types were identified, although the percentage of immune cells of all living cells in TC tumours was relatively low.

## 2 | MATERIALS AND METHODS

### 2.1 | Ethics statement

All samples included in this study were donated by patients undergoing surgical removal of lung cancer at Oslo University Hospital in the period from February 2014 to June 2015. The study was approved by the Regional Committee

for Medical and Health Research Ethics (Oslo, Norway, ref. S-05307). All participants included in the study have signed written informed consent.

### 2.2 | Patients and clinical material

Included patients underwent surgery with lobectomy at the Department of Cardiothoracic Surgery at Rikshospitalet and Ullevål hospitals, Oslo University Hospital, Oslo, Norway. The histopathological criteria for TC diagnosis were those of the 2015 World Health Organization classification, that is a tumour having carcinoid morphology, less than 2 mitoses per 2 mm<sup>2</sup>, no necrosis and a size of 0.5 cm or larger.<sup>1,2</sup> A sample of the tumour, non-cancerous distal lung tissue, lymph node and blood were collected from four patients. Tumour, distal lung and lymph node were sampled after the lobe had been extracted from the patient. Tumour tissue was sampled by cutting through the central mass of the tumour. Non-cancerous lung tissue was sampled furthest away from the tumour in the resected lobe and designated 'distal lung'. From one patient, half a lymph node was sampled from station 10 (around the bronchus), following the European guidelines for lung cancer surgery.<sup>19</sup> Blood was sampled from the central venous catheter after the patient was anesthetized, but before the surgery started. Tumour, distal lung and lymph node samples were transported on ice in transport media (DMEM, Gibco, cat-no. 10565-018, with 0.25 µg/mL amphotericin, Sigma-Aldrich, cat-no. A2942). Blood was transported at room temperature in EDTA tubes. To obtain a single cell suspension, tumour, distal lung and lymph node were mechanically dissociated separately using scissors, and incubated with digestion media (consisting of DMEM supplemented with 2 mg/mL collagenase A, Roche, cat-no. 10103586001 and 50 units/mL DNase, Roche, cat-no. 11284932001) at 37°C for 1 hour, with stirring magnet. The digested tissues were filtered through 100-µm filter (Falcon, cat-no. 35236) to remove debris, centrifuged at 410 g for 6 minutes at 4°C, and the cell pellets were resuspended in PBS with 10% FBS (Sigma, cat-no. F7524). The blood was processed using a density gradient (Lymphoprep, Axis-Shield, cat-no. 07811) to obtain peripheral blood mononuclear cells (PBMCs).

### 2.3 | Flow cytometry

Single cell suspensions from tumour, distal lung, lymph node and PBMCs were analysed using six different flow cytometry panels (Tables S1-S6). The cell suspensions were incubated with 12.5 µg/mL mouse IgG (Sigma, cat-no. I8765-10MG) in 96-well plates (Corning, Costar, cat-no. 3894) for 15 minutes, on ice, in the dark, to block unspecific binding of antibodies. Cells were further incubated with fluorochrome-conjugated monoclonal antibodies for 30 minutes on ice in the dark. Following

the incubation, 100  $\mu$ L of flow buffer was added to each well, and the plates were centrifuged at 410 g for 6 minutes at 4°C. Supernatants were discarded, and cell pellets were resuspended in 150  $\mu$ L flow buffer per well and centrifuged again (410 g for 6 minutes at 4°C). The cell pellets were resuspended in 200  $\mu$ L of flow buffer, filtered through a 100  $\mu$ m mesh (Falcon, cat-no. 352360) and stained with 5  $\mu$ g/mL propidium iodide (PI) immediately before analysis on BD LSRFortessa flow cytometer (BD Bioscience). Data were analysed using FlowJo V10 software (FlowJo, LLC). Positive gates were set on the basis of the signal from isotype-matched control antibodies.

## 2.4 | Statistics

Statistical calculations were performed using GraphPad Prism 8.0 (GraphPad). Statistical significance was calculated using a two-tailed Mann-Whitney test. *P*-value <.05 was considered significant.

## 3 | RESULTS

### 3.1 | Leucocytes infiltrate TC tumours to a lower degree compared to distal lung

In order to characterize the immune cell composition in TC tumours, we analysed fresh samples from tumour, non-cancerous distal lung, lymph node and blood from four female never-smoker TC patients with a mean age of 58.8 years (Table 1). We used six different flow cytometry panels (Tables S1-S6) that we developed in a previous study of NSCLC.<sup>13</sup> Single cell suspensions were generated from four tumours and four distal lung samples by dissection, mechanical dissociation and enzymatic digestion. From one patient, a sample from a lung draining lymph node was collected. Due to limited sample availability, each patient was typically analysed with only 2-3 flow cytometry panels. To identify immune cells, we devised a gating strategy presented in Figure 1A-D. This gating method excluded debris on the basis of size in a FSC-A (forward scatter area) and SSC-A (side scatterarea) dot plot (Figure 1A), excluded cell doublets and clumps as FSC-H (Height)/FSC-A off-diagonal events (Figure 1B) and excluded PI-positive dead cells (Figure 1C). Thereafter, the leucocytes were identified as CD45<sup>+</sup> cells (Figure 1D). The percentages of leucocytes in tumour were calculated as the fraction of all live cells (as defined in Figure 1C). In this TC patient cohort, CD45<sup>+</sup> leucocytes represented on average 24% of all live cells in tumour and 62% of all live cells in distal lung (Figure 1E). The percentage of tumour-infiltrating leucocytes varied considerably between patients (from 6.1% to 44.1%), but was consistently and significantly (*P* = .028) lower than in distal lung (Figure 1E). Thus, a modest leucocyte infiltrate was observed in all four TC tumours investigated.

### 3.2 | Most T cells in TC tumours have an effector/memory phenotype

The T-cell composition was examined in tumour samples from two TC patients. The leucocyte population was first defined as single, live, CD45<sup>+</sup> cells (as shown in Figure 1A-D). Thereafter, we identified lymphocytes based on their size and granularity (Figure 2A). From this population, CD19<sup>+</sup> B cells were excluded (Figure 2B) and the CD3 marker was used to identify T cells (Figure 2C). Three T-cell subpopulations were observed in TC tumours: CD4<sup>+</sup> T cells, CD8<sup>+</sup> T cells and CD4<sup>-</sup>CD8<sup>-</sup> double-negative T cells (Figure 2D). CD3<sup>+</sup> T cells represented on average 39.5% (range 16-63) of all tumour-infiltrating leucocytes, which was similar to the average T-cell frequency in distal lung (43.5%, Figure 2E). CD4<sup>+</sup> T cells in TC tumours constituted 17.7% (range 7.3-28.1) of all tumour-infiltrating leucocytes while CD8<sup>+</sup> T cells constituted 19.8% (range 6.4-33.2). The double-negative CD4<sup>-</sup>CD8<sup>-</sup> T-cell population only represented 0.9% of tumour-infiltrating leucocytes (Figure 2F). CD8<sup>+</sup> T cells constituted 46.2% of all CD3<sup>+</sup> T cells, whereas CD4<sup>+</sup> T cells constituted 44.5%. The CD4<sup>-</sup>CD8<sup>-</sup> cells represented 1.65% of all T cells (Figure 2G, H). A similar distribution of T-cell

**TABLE 1** Patient population characteristics

Characteristics	Number (%)
Histopathology	
Typical carcinoid tumour	4 (100%)
Age	
Mean	58.8
Range	36-75
Stage	
IA	1 (25%)
IB	3 (75%)
Gender	
Female	4 (100%)
Male	0
Tumour location	
Right middle lobe	2 (50%)
Left lower lobe	2 (50%)
Procedure	
Lobectomy	2 (50%)
Bilobectomy	2 (50%)
Smoking history	
Smoker	0
Never Smoker	4 (100%)
Concomitant disease	
No disease	3 (75%)
Mild emphysema	1 (25%)

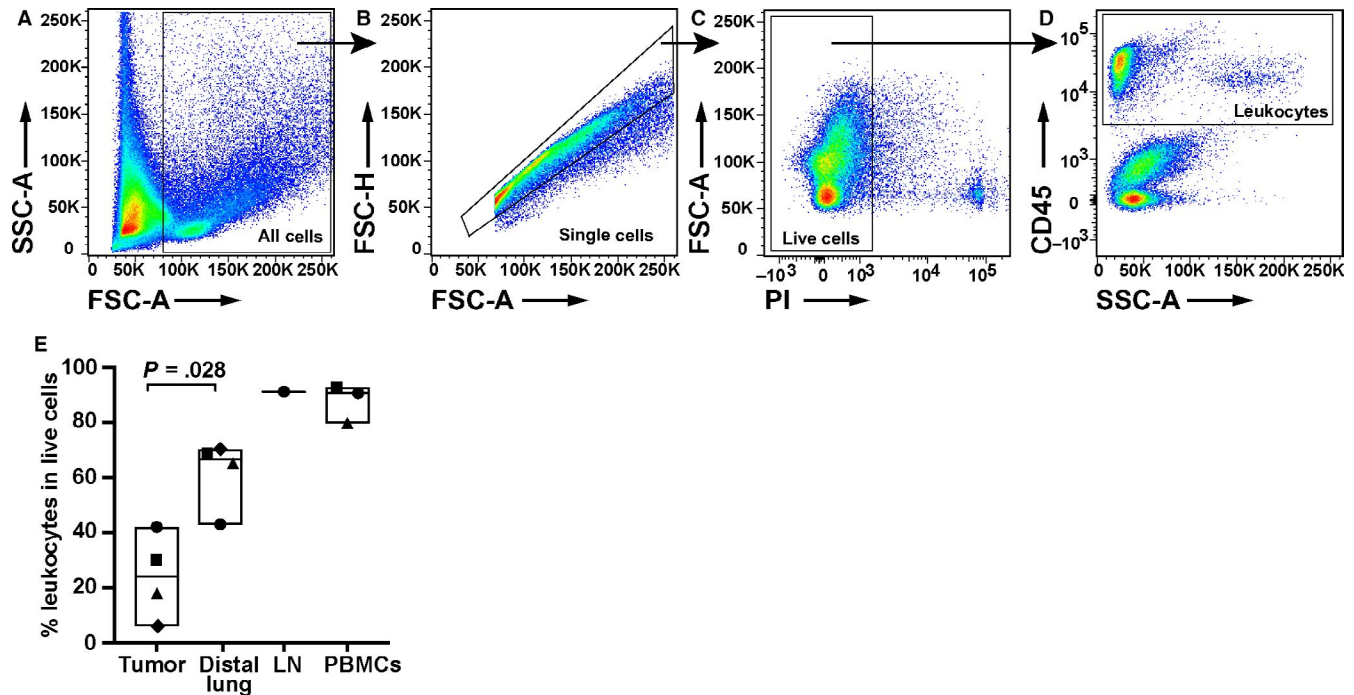


**FIGURE 1** Identification of leucocytes in tissues from four patients with typical carcinoid. The proportion of live CD45<sup>+</sup> leucocytes was determined by flow cytometry using the same gating strategy on tumour tissue, distal lung, lymph node and PBMCs. A, All events acquired by flow cytometry were first observed in a side scatter (SSC) and forward scatter (FSC) plot, and the size of the events (FSC-A) was used to exclude debris and define all cells. B, The cells gated in A ('all cells') were observed in FSC height (H) and FSC area (A) plot to exclude doublets and identify single cells. C, Dead cells were excluded from the single cell population using propidium iodide (PI), which labels dead cells. D, Within the population of single, live cells, leucocytes were identified using the marker CD45. E, The graph shows leucocytes as a fraction of all live cells in TC tumour, distal lung, lymph node and PBMCs. Each symbol represents data from one patient (n = 4). Mann-Whitney test was used for statistical comparison of the two groups tumour and distal lung. LN, lymph node

subpopulations was observed in distal lung. In contrast, PBMCs from one patient were dominated by CD4<sup>+</sup> T cells (Figure 2H) in accordance with blood from healthy donors as previously reported.<sup>20</sup>

Examination of TCR type in a TC tumour from one patient revealed that most CD4<sup>+</sup> and CD8<sup>+</sup> T cells expressed the  $\alpha\beta$ TCR (99.4 and 98.1%, respectively) (Figure 2I,J). In contrast and interestingly, most CD4<sup>-</sup>CD8<sup>-</sup> T cells were negative for this TCR type (64.4%), suggesting that they may represent  $\gamma\delta$ T cells (Figure 2K,L). The naïve/memory phenotype of CD4<sup>+</sup>, CD8<sup>+</sup> and CD4<sup>-</sup>CD8<sup>-</sup> T cells in TC tumour was analysed in two patients. The majority of CD4<sup>+</sup> and CD8<sup>+</sup> T cells had an effector/memory (CD45RA<sup>-</sup>CD45RO<sup>+</sup>) phenotype (79.5% and 79.9%, respectively, Figure 2M,N), with the remainder exhibiting a naïve (CD45RA<sup>+</sup>CD45RO<sup>-</sup>) phenotype. In contrast, CD4<sup>-</sup>CD8<sup>-</sup> T cells consisted of similar fractions of memory and naïve cells (Figure 2O,P). Distal lung T cells had a similar distribution of naïve vs. effector memory phenotypes as the tumour, whereas T cells in blood were mostly naïve cells (Figure S1). Taken together, the data show that T cells are present in TC tumours and constitute a large proportion of the infiltrating leucocytes. These T cells express mainly the  $\alpha\beta$ TCR and mostly harbour an effector/memory phenotype.

### 3.3 | TC tumours contain both naïve and memory B cells

B cells were investigated in TC tumours from three patients. In one patient, the B-cell subset composition was examined in more detail. B cells were defined among leucocytes as CD19<sup>+</sup>CD14<sup>-</sup>CD3<sup>-</sup> cells (Figure 3A-C). Among all B cells, we identified CD27<sup>+</sup> (black square) and IgD<sup>+</sup> populations (brown square) (Figure 3D). Both populations were further examined for the expression of IgM and CD38 markers (Figure 3E,F). Within the IgD<sup>+</sup> population, the majority of cells (97.5%) were IgM<sup>+</sup> naïve B cells (Figure 3E). Within the CD27<sup>+</sup> population, three subpopulations were identified: CD38<sup>++</sup>IgM<sup>-</sup> plasma cells, CD38<sup>±</sup>IgM<sup>-</sup> memory B cells and CD38<sup>±</sup>IgM<sup>+</sup> IgM-positive memory B cells (Figure 3F). The single TC tumour investigated contained 31.1% (of all B cells) class-switched IgM<sup>-</sup> memory B cells and 15% IgM<sup>+</sup> memory B cells. Naïve B cells were the next most abundant population (35% of all B cells), followed by plasma cells (3.9% of B cells) (Figure 3G). CD19<sup>+</sup> B cells constituted on average 11.5% of all immune cells in TC tumour, with a large patient-to-patient variation (from 2.5% to 20.7%) (Figure 3H). In distal lung, B cells comprised 4.5% of the leucocyte population (range 1.3-8) (Figure 3H). Thus,



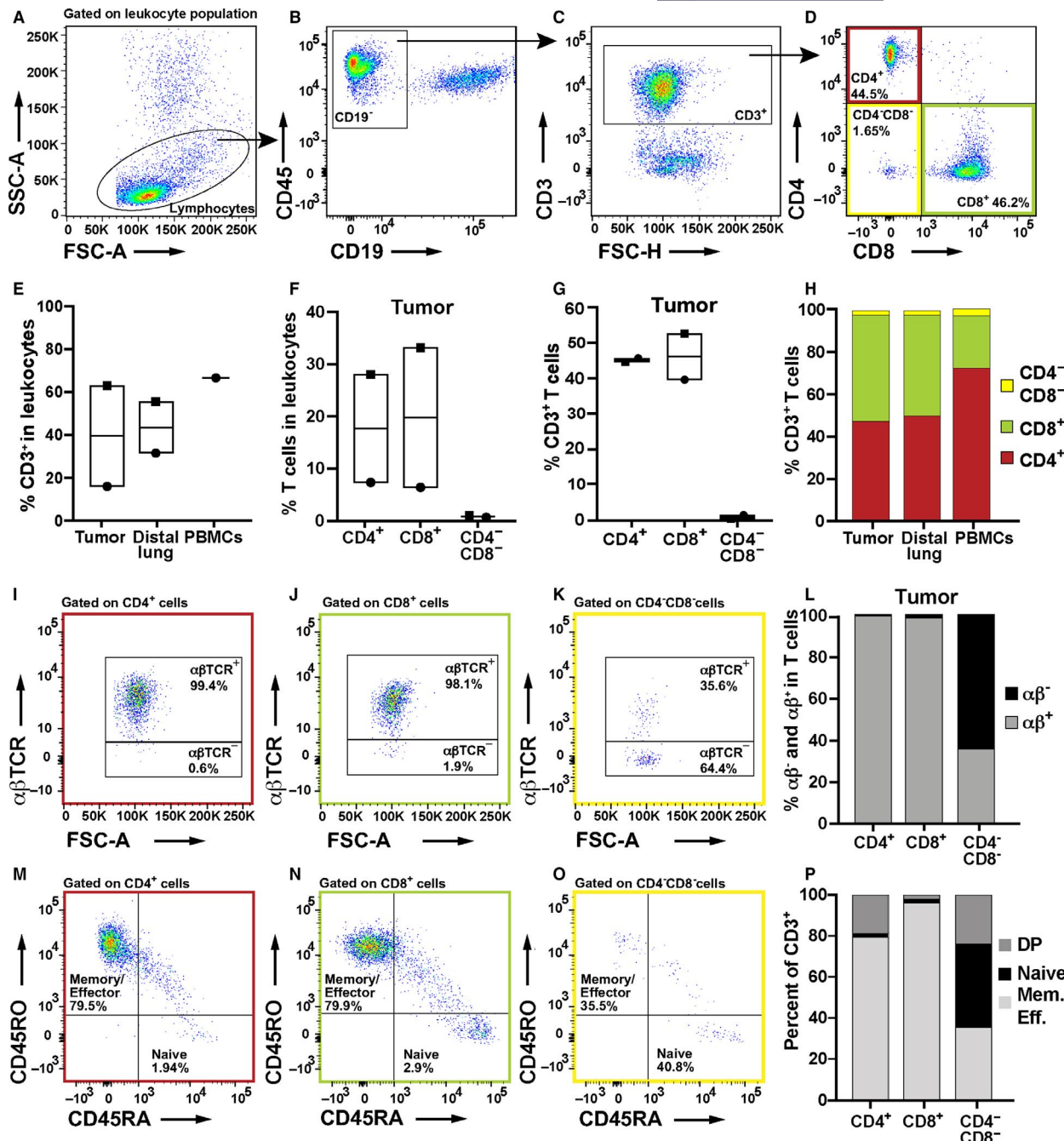


**FIGURE 2** T-cell infiltration in typical carcinoid tumours. A, The FSC-SSC plot shows live, single CD45<sup>+</sup> leucocytes which were gated as presented in Figure 1 A-D. Within this leucocyte population, a lymphocyte gate was set based on cell size (FSC) and granularity (SSC). B, CD19<sup>+</sup> B cells were excluded from further analysis. C, The CD19<sup>-</sup> population was examined for CD3<sup>+</sup> T cells. D, CD3<sup>+</sup> T cells could be divided in three distinct subpopulations based on the expression of CD4 and CD8: CD4<sup>+</sup> T cells, CD8<sup>+</sup> T cells and CD4<sup>-</sup>CD8<sup>-</sup> T cells. The percentages displayed in the quadrants represent the average proportion of each subpopulation among the gated CD3<sup>+</sup> T cells (n = 2). E, Percentages of CD3<sup>+</sup> T cells among CD45<sup>+</sup> leucocytes in two patients (n = 2). F, Percentages of CD4<sup>+</sup> T, CD8<sup>+</sup> T and CD4<sup>-</sup>CD8<sup>-</sup> T cells among CD45<sup>+</sup> leucocytes infiltrating TC tumours (n = 2). G, Proportions of CD4<sup>+</sup> T, CD8<sup>+</sup> T and CD4<sup>-</sup>CD8<sup>-</sup> T cells among CD3<sup>+</sup> T cells in TC tumours (n = 2). H, Distribution of CD4<sup>+</sup> T, CD8<sup>+</sup> T and CD4<sup>-</sup>CD8<sup>-</sup> T cells in tumour, distal lung and PBMCs from two patients with TC. The T-cell subpopulations defined in panel D were examined for expression of the αβ T-cell receptor (TCR). I, TCR characteristics of the CD4<sup>+</sup> T cells. J, TCR characteristics of the CD8<sup>+</sup> T cells. K, TCR characteristics of the CD4<sup>-</sup>CD8<sup>-</sup> T cells. The percentages in panels I-K show data from TC tumour of one patient. L, Distribution of αβ<sup>+</sup> and αβ<sup>-</sup> T cells in the indicated subpopulations (n = 1). M-O, The phenotype of the T-cell subsets was examined using CD45RO, a memory marker and CD45RA, a marker of naive cells. M, Phenotype of CD4<sup>+</sup> T cells in TC tumour. N, Phenotype of CD8<sup>+</sup> T cells in TC tumour. O, Phenotype of CD4<sup>-</sup>CD8<sup>-</sup> T cells in TC tumour. Percentages in panels M-O are average values for TC tumour from two patients. P, Proportions of memory (light grey), naive (black) and double-positive (DP) T cells among the indicated T-cell subsets, shown as mean values of TC tumour from two patients

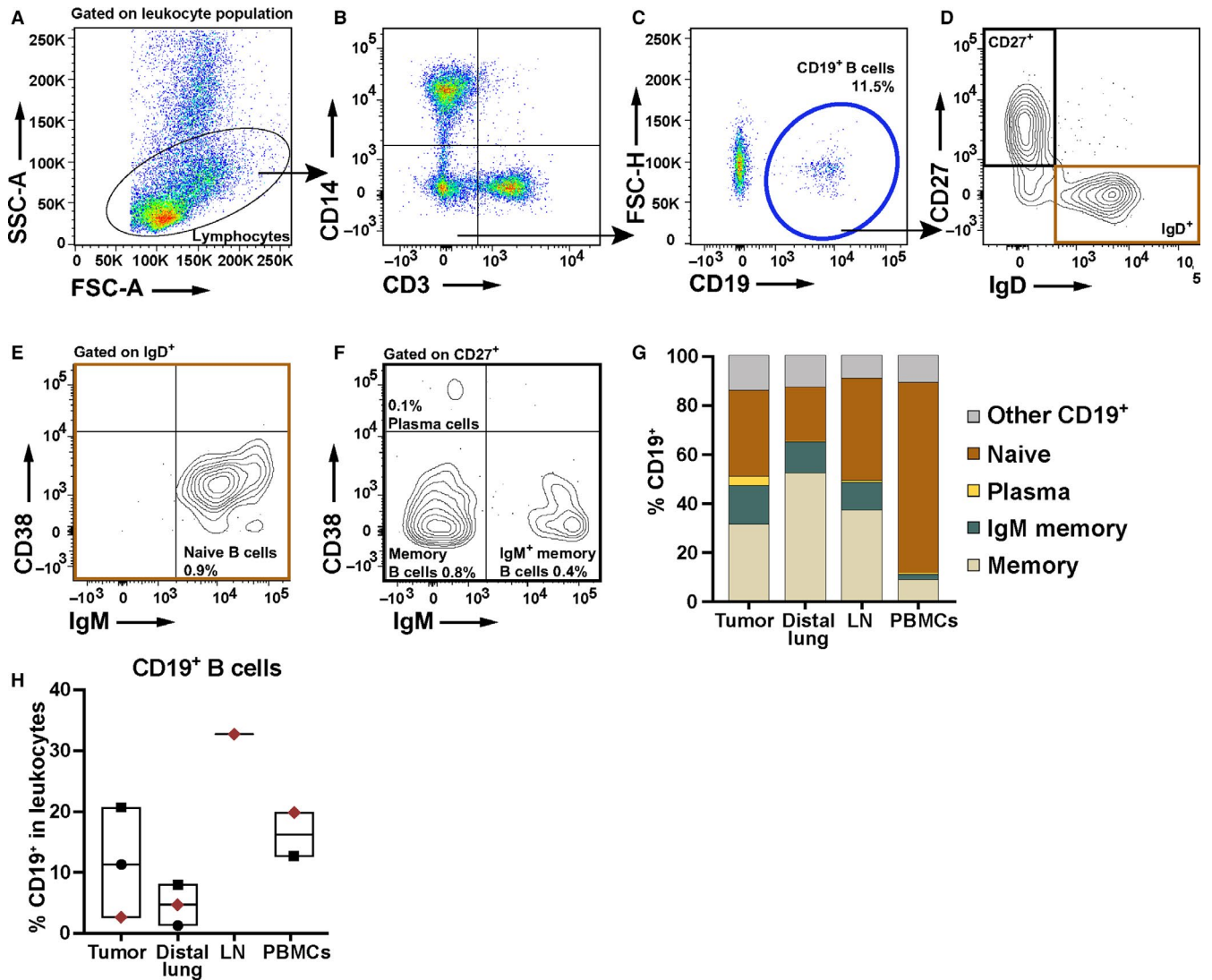


**FIGURE 3** B cells and B-cell subsets in typical carcinoid tumour. A, The plot shows live, single CD45<sup>+</sup> leucocytes gated as presented in Figure 1A-D. Within this leucocyte population, a lymphocyte gate was defined based on the size (FSC) and granularity (SSC) of the cells. B, T cells (CD3<sup>+</sup>) and macrophages (CD14<sup>+</sup>) were excluded from the lymphocyte gate. C, Within the CD3<sup>-</sup>CD14<sup>-</sup> population, B cells were identified as CD19<sup>+</sup>. D, All CD19<sup>+</sup> B cells were further divided based on IgD and CD27 expression. E, The IgD expressing B cells co-expressed IgM and were therefore defined as naive B cells (n = 1). F, The CD27<sup>+</sup> B cells were examined for CD38 and IgM expression. The cells expressing only CD38 are defined as plasma cells, whereas cells expressing only IgM are IgM<sup>+</sup> memory B cells. The double-negative (CD38<sup>-</sup>IgM<sup>-</sup>) cells were defined as memory B cells (n = 1). The percentages in panel E and F show the values for each B-cell subset within the CD45<sup>+</sup> leucocyte population (n = 1). G, Proportions of B cell subsets within the CD19<sup>+</sup> population in tissues from one patient with TC. H, Percentages of CD19<sup>+</sup> B cells in tissues from patients diagnosed with TC tumour. Each symbol represents data from one patient (n = 3). The red symbol shows the patient tissues that were analysed for B cell subsets presented in panel E-G. LN, lymph node

CD19<sup>+</sup> B cells are present in TC tumour, mostly in the form of naive and memory B cells.

### 3.4 | Innate APC subpopulations in TC tumours

The professional innate APC compartment (DCs and macrophages) was characterized in TC tumours from two patients. We first excluded CD19<sup>+</sup> B cells from the leucocytes (Figure 4A) and gated the remaining HLA-DR<sup>+</sup> cells

(Figure 4B). Among the CD19<sup>-</sup>HLA-DR<sup>+</sup> cells, macrophages were defined as CD14<sup>+</sup> cells and myeloid DCs as CD11c<sup>+</sup>CD14<sup>-</sup> cells (Figure 4C). Among CD11c<sup>-</sup>CD14<sup>-</sup> cells, CD123<sup>+</sup> cells were defined as plasmacytoid DCs (pDCs, Figure 4D). The CD11c<sup>+</sup>CD14<sup>-</sup> myeloid DC population was divided into three subpopulations based on CD141 and CD1c expression: CD1c<sup>+</sup> DCs, CD141<sup>+</sup> DCs and a double-negative (DN) DC subset (Figure 4E). Within TC tumours, the combined four DC subpopulations identified made 3.1% of all leucocytes. The highest frequency in TCs was observed by DN DCs (1.8%), followed by CD1c<sup>+</sup> DCs (0.7%)

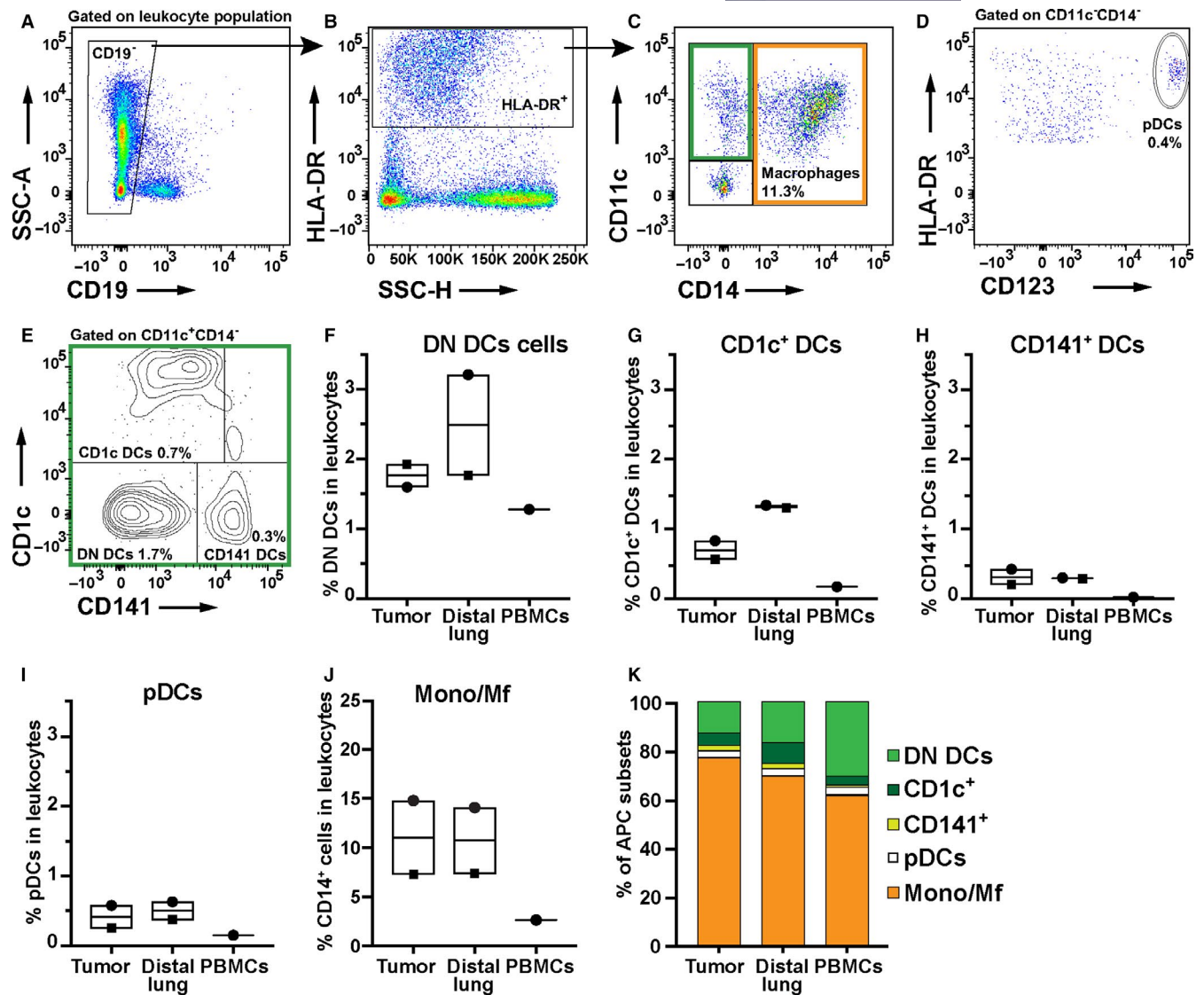


**FIGURE 4** Macrophages and DCs infiltrate typical carcinoid tumours. A, The plot shows live, single CD45<sup>+</sup> leucocytes obtained by the gating strategy described in Figure 1A-D. Within this leucocyte population, CD19<sup>+</sup> cells were excluded, and only CD19<sup>-</sup> cells were used in further analysis. B, CD19<sup>-</sup> cells were divided into HLA-DR<sup>+</sup> and HLA-DR<sup>-</sup> cells. Only those that were HLA-DR<sup>+</sup> were used in further analyses for identification of APCs. C, HLA-DR<sup>+</sup> cells were examined for expression of CD14 and CD11c, and CD14<sup>+</sup> cells are defined as monocytes/macrophages. D, CD14<sup>-</sup>CD11c<sup>-</sup> cells were examined for CD123 expression, and CD123<sup>+</sup> cells were defined as plasmacytoid DCs (pDCs) (n = 2). E, HLA-DR<sup>+</sup>CD11c<sup>+</sup>CD14<sup>-</sup> cells were examined for expression of CD1c and CD141, which revealed the presence of three DC populations in tissues from TC patients: CD1c<sup>+</sup> DCs, CD141<sup>+</sup> DCs, and CD1c and CD141 double-negative (DN) DCs (n = 2). F-I, Percentages of four DC subsets among the CD45<sup>+</sup> leucocyte population of patients with TC tumour: % DN DCs (F), % CD1c<sup>+</sup> DCs (G), % CD141<sup>+</sup> DCs (H) and % pDCs (I). J, Proportions of HLA-DR<sup>+</sup>CD14<sup>+</sup> macrophages in tumour and non-cancerous distal lung tissue, and HLA-DR<sup>+</sup>CD14<sup>+</sup> monocytes in PBMCs shown in per cent of the CD45<sup>+</sup> leucocyte population. K, APC subsets are shown in percentage, calculated from the total number of APCs (CD19<sup>-</sup>HLA-DR<sup>+</sup> cells) in patients with TC (n = 2). In panels F-J: Each symbol represents data from one patient (n = 2)

and CD141<sup>+</sup> DCs (0.3%) (Figure 4F-H). It should be noted that the DN DC population may consist of a mixture of DCs and CD14-negative macrophages.<sup>13</sup> The pDCs constituted on average 0.4% of total leucocytes (Figure 4I). Macrophages were consistently the largest professional APC population in TC tumours, constituting on average 11% (range from 7.3% to 14.8%) of all leucocytes (Figure 4J,K). The percentages of DCs and macrophages were similar in distal lung and TC tumours. Thus, TC tumours contain both macrophages and at

least three distinct DC subpopulations (CD1c<sup>+</sup> DCs, CD141<sup>+</sup> DCs and pDCs).

### 3.5 | The majority of NK cells in TC tumours express CD16

To investigate whether NK cells were present in TC tumours, we first identified the leucocytes (as shown in Figure 1A-D),



and made a lymphocyte gate (Figure 5A). CD19<sup>+</sup> B cells and CD14<sup>+</sup> macrophages were excluded from the lymphocyte population (Figure 5B,C). The remaining cells were plotted in a CD56 versus CD3 dot plot, identifying three populations: CD3<sup>+</sup> T cells, the CD3<sup>-</sup>CD56<sup>+</sup> NK cells and a double-positive CD3<sup>+</sup>CD56<sup>+</sup> population (Figure 5D). The CD3<sup>+</sup>CD56<sup>+</sup> double-positive population may consist of either *bona fide* NK T cells or classical T cells expressing the CD56 marker. Based on CD16 expression, the CD56<sup>+</sup> NK cells were further divided in two subsets: CD16<sup>+</sup> and CD16<sup>-</sup> NK cells (Figure 5E).

The CD56<sup>+</sup> NK cells made, on average, 8.8% (range 6-11.7) of all immune cells in TC tumour with CD16<sup>+</sup> cells

constituting 6.4% and CD16<sup>-</sup> cells constituting 2.4% of all leucocytes (Figure 5F-H). The distribution of CD16 expression on NK cells in TC tumour, as well as in distal lung, was skewed towards CD16 positivity (Figure 5J).

### 3.6 | Granulocytes are present in TC tumours

The presence of granulocytes was investigated in the tumour from one TC patient. Leucocytes were first defined as shown in Figure 1A-D. From the leucocyte population,

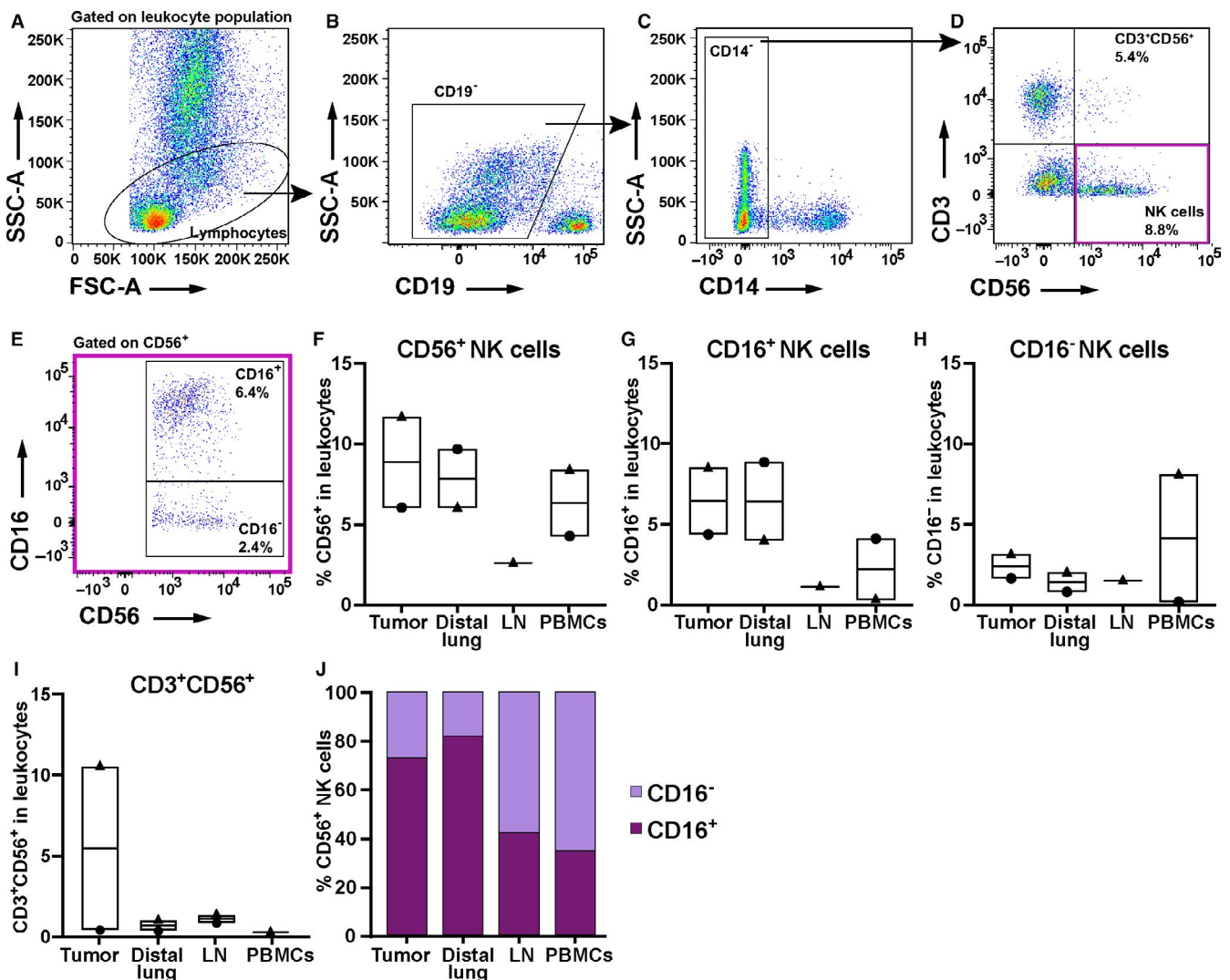


**FIGURE 5** Presence of different NK cell subsets in typical carcinoid tumour. A, The plot shows live, single CD45<sup>+</sup> leucocytes obtained by using the gating strategy presented in Figure 1A-D. Within this leucocyte population, a lymphocyte gate was set based on cell size and granularity. B, CD19<sup>+</sup> B cells were excluded from the lymphocyte population. C, CD14<sup>+</sup> macrophages were excluded from the CD19<sup>-</sup> population. D, The remaining cells were examined for expression of CD3 and CD56, and three populations were identified: CD3<sup>+</sup>CD56<sup>-</sup> T cells, CD3<sup>+</sup>CD56<sup>+</sup> cells and CD3<sup>-</sup>CD56<sup>+</sup> NK cells (n = 2). E, The CD56<sup>+</sup> NK cells could be divided into two subsets based on CD16 expression: CD16<sup>+</sup> and CD16<sup>-</sup> NK cells. The percentages in panels D and E show the proportion of the indicated population within the CD45<sup>+</sup> leucocyte population (n = 2). F-H, Percentages of NK cells in the CD45<sup>+</sup> leucocyte population of patients with TC tumour: (F) CD56<sup>+</sup> NK cells, (G) CD56<sup>+</sup>CD16<sup>+</sup> NK cells and (H) CD56<sup>+</sup>CD16<sup>-</sup> NK cells. I, The percentage of CD3<sup>+</sup>CD56<sup>+</sup> cells among CD45<sup>+</sup> leucocytes in different tissues from patients with typical TC tumour. J, Distribution of CD16<sup>+</sup> and CD16<sup>-</sup> CD56<sup>+</sup> NK cells in two patients. In panels F-I, each symbol represents data from one patient (n = 2). LN, lymph node



CD14<sup>+</sup> macrophages, CD3<sup>+</sup> T cells and CD19<sup>+</sup> B cells were excluded (Figure 6A). The resulting population was then analysed for the expression of CD11b (Figure 6B). Cells expressing CD11b were further analysed for expression of CD15 (Figure 6C), while cells lacking CD11b were analysed for expression of FcεR1 (Figure 6D). The FcεR1<sup>+</sup> cells were analysed for expression of CD49d and CD117 in order to identify CD117<sup>+</sup>CD49d<sup>+</sup> mast cells and CD117<sup>-</sup>CD49d<sup>+</sup> basophils (Figure 6E). The CD11b<sup>+</sup> cells that expressed CD15 were analysed for expression of CD49d to define CD49d<sup>-</sup> neutrophils and CD49d<sup>+</sup> eosinophils (Figure 6F). The predominant population of granulocytes in the TC tumour was the neutrophils constituting 3.9% of all leucocytes, followed by the basophils (1.2%), mast cells (0.8%) and eosinophils (0.6%) (Figure 6G). In

the distal lung, neutrophils were the most abundant population (8.9%), while the basophils, mast cells and eosinophils were minor populations. Compared to the distal lung, the TC tumour examined had a lower frequency of neutrophils but a higher frequency of other granulocyte subsets (Figure 6H). Thus, all four granulocyte subsets (neutrophils, basophils, eosinophils and mast cells) can be found in TC tumour.

### 3.7 | The immune landscape of TC tumours is similar to that of non-cancerous lung

As summarized in Figure 7A, we found that tumour-infiltrating leucocytes in TC tumours were dominated by T cells

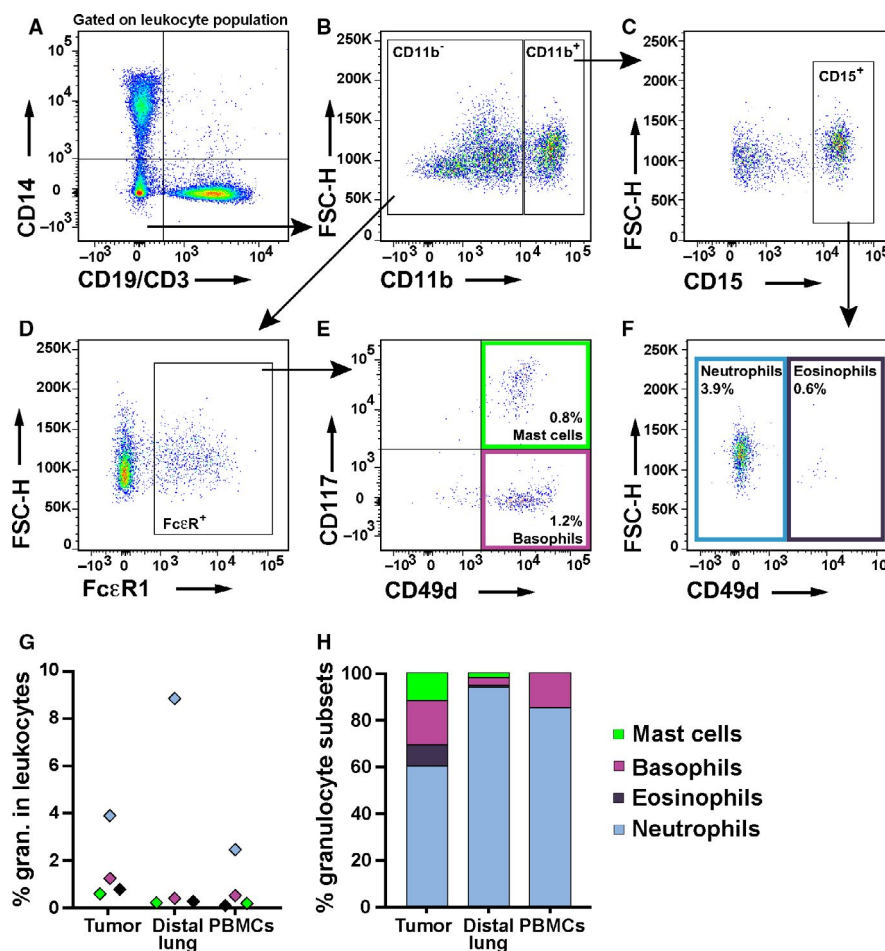


**FIGURE 6** All granulocyte populations were identified in typical carcinoid tumour. A-F The gating strategy that was used to identify granulocytes in tissues from patients with TC tumour. A, The plot shows the leucocyte population obtained by using the gating strategy described in Figure 1A-D. The leucocyte population was analysed for expression of CD14, CD19 and CD3. CD14<sup>+</sup> macrophages, CD19<sup>+</sup> B cells and CD3<sup>+</sup> T cells were excluded from further analysis. (B) The remaining cells were divided into CD11b<sup>+</sup> and CD11b<sup>-</sup> cells. (C) CD11b<sup>+</sup> cells were examined for expression of CD15. (D) The CD11b<sup>-</sup> cells were analysed for FcεR1 expression. (E) FcεR1<sup>+</sup> cells were assessed for expression of CD117 and CD49d, and were divided into CD117<sup>+</sup>CD49d<sup>+</sup> mast cells and CD117<sup>-</sup>CD49d<sup>+</sup> basophils (n = 1). (F) CD15<sup>+</sup> cells were analysed for expression of CD49d, and divided into CD49d<sup>+</sup> eosinophils and CD49d<sup>-</sup> neutrophils (n = 1). Percentages in panels E and F show the proportion of the given population within the CD45<sup>+</sup> leucocyte population (n = 1). (G) Distribution of neutrophils, eosinophils, basophils and mast cells calculated from the total number of CD45<sup>+</sup> leucocytes in tumour, non-cancerous distal lung and PBMCs from one patient with TC. (H) Percentages of various granulocyte populations in relation to the total number of granulocytes (n = 1). All data presented in panels A-H were obtained from one single patient

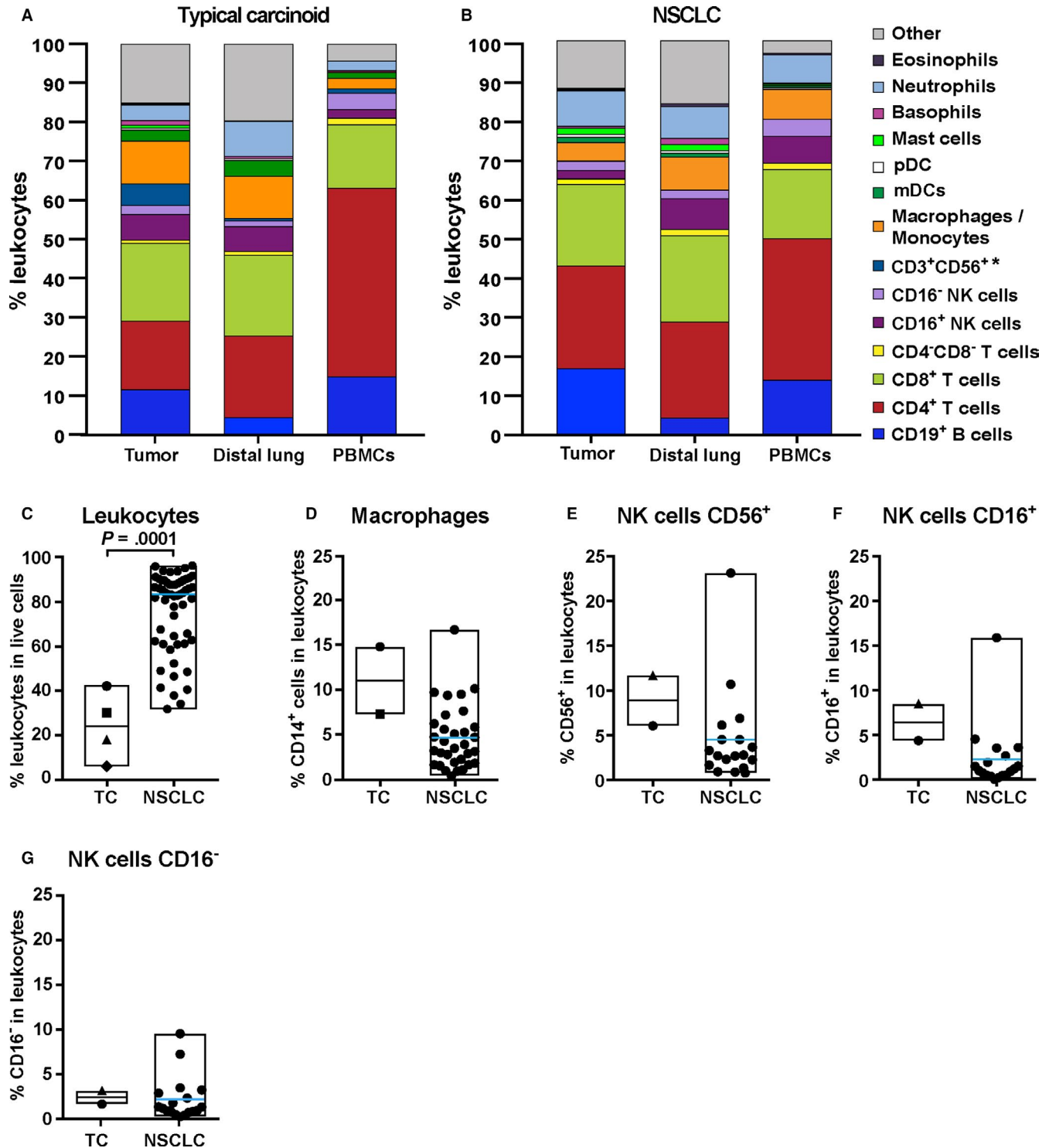


**FIGURE 7** Comparison of immune cell composition in typical carcinoid and NSCLC. **A**, The bar graph shows the immune cell composition in TC tumour, distal lung and PBMCs in the never-smoking female patients presented in this study. Percentages for each cell population represent mean values based on data collected for the respective cell type in the indicated tissue. **B**, The bar graph shows immune cell composition in NSCLC, distal lung and PBMCs from 69 patients presented in previously published work (Figure adapted from<sup>13</sup>). Percentages of each cell population represent mean values based on data collected for the respective cell population in the indicated tissue. The symbol \* indicates that CD3<sup>+</sup>CD56<sup>+</sup> cells were analysed in TC tumour but not in NSCLC. **C**, The percentage of CD45<sup>+</sup> leucocytes among all live cells analysed in TC and NSCLC tumours. Mann-Whitney test was used for statistical comparison of the two groups. **D-G**, Comparison of the frequency of cellular subsets identified in tumours from patients with TC or NSCLC: **(D)** HLA-DR<sup>+</sup>CD14<sup>+</sup> macrophages, **(E)** CD56<sup>+</sup> NK cells, **(F)** CD56<sup>+</sup>CD16<sup>+</sup> NK cells and **(G)** CD56<sup>+</sup>CD16<sup>-</sup> NK cells. The percentages were calculated from the total number of CD45<sup>+</sup> leucocytes. Each symbol represents data from one patient. All data from NSCLC have been previously reported<sup>13</sup>

(39.5%), followed by almost equal percentages of B cells (11.5%) and macrophages (11%). At least three DC subsets were identified: CD1c<sup>+</sup> DCs (0.7%), CD141<sup>+</sup> DCs (0.3%) and pDCs (0.4%). We further described NK cells (8.8%) of which the majority expressed the CD16 marker (6.4%), as well as a population of CD3<sup>+</sup>CD56<sup>+</sup> cells (5.4%). Finally, all four granulocytes populations were observed in TC tumours: neutrophils (3.9%), basophils (1.2%), mast cells (0.8%) and eosinophils (0.6%). The immune cell composition of TC tumour appears quite similar to that of the non-cancerous distal lung (Figure 7A).

Finally, we wished to compare the immune cell composition of TC versus NSCLC tumours (adenocarcinoma and squamous cell carcinoma) using a cohort of 69 NSCLC patients previously analysed by our laboratory (Figure 7B).<sup>13</sup> In general, TC and NSCLC tumours had a similar and complex immune landscape, with CD3<sup>+</sup> T cells representing the largest population of immune cells. Both tumour types contained B cells, NK cells, macrophages, myeloid DCs, pDC and granulocytes (Figure 7A,B). Nevertheless, there were significant differences in the immune infiltrate. The most notable was the percentage of tumour-infiltrating CD45<sup>+</sup> leucocytes. In TC tumours, CD45<sup>+</sup> leucocytes comprise, on average, 24% of all live cells, which is significantly lower than in NSCLC tumours ( $P = .0001$ ) (Figure 7C). Within all leucocytes, macrophages seemed to constitute a rather large population in TC compared to NSCLC (Figure 7D). Further potential differences concern the infiltration of CD56<sup>+</sup> NK cells (Figure 7E-G).

## 4 | DISCUSSION

In this study, we characterized the composition and frequency of tumour-infiltrating leucocytes of four never-smoker TC patients using multiparametric flow cytometry. The percentage of CD45<sup>+</sup> leucocytes (of all living cells) in TC tumour was lower compared to non-cancerous distal lung, but the general composition was similar. As an important technical note, virtually all CD4<sup>+</sup> and CD8<sup>+</sup> T cells in TC tumours had an effector/memory (CD45RA<sup>-</sup>CD45RO<sup>+</sup>) phenotype, indicating that blood contamination in tumour samples was negligible, because most T cells in blood have a naïve CD45RA<sup>+</sup>CD45RO<sup>-</sup> phenotype.<sup>13</sup> TC tumours were found to contain at least twelve different types of immune cells: CD4<sup>+</sup> T cells, CD8<sup>+</sup> T cells, B cells, macrophages, CD1c<sup>+</sup> DCs, CD141<sup>+</sup> DCs, pDCs, NK cells and four subsets of granulocytes, namely neutrophils, basophils, eosinophils and mast cells.

To the best of our knowledge, our data represent the first detailed characterization of the immune cell composition in low-grade TC tumours. Previously, Vesterinen et al reported low numbers of PD-1-positive lymphocytes in some, but not all, TC tumours examined.<sup>17</sup> The only immune cell

type previously identified with certainty in TC tumours are the cytotoxic CD8<sup>+</sup> T cells.<sup>15-17</sup> Katsenelson et al failed to detect DCs (using the CD1a<sup>+</sup> and CD83<sup>+</sup> markers) in bronchial carcinoid tumours.<sup>18</sup> In contrast, the immune cell composition of high-grade lung cancers, such as NSCLC, has been described in detail.<sup>11,13</sup> Notably, the percentage of leucocytes (of all living cells) in NSCLC tumours was higher compared to distal lung.<sup>13</sup> This is contrary to our findings in TC and indicates different relation of the immune system to these two types of tumours. The level of inflammation appears to be relatively low in TC and high in NSCLC tumours. Several features of TC tumours may potentially contribute to the induction of a weaker immune response, as compared to NSCLC, such as a low mutational load, a very slow progression and the absence of central necrotic areas in TC tumours.

## ACKNOWLEDGMENT

Authors would like to thank Ingerd Solvoll for invaluable support with biopsy procurement.

## CONFLICT OF INTEREST

Authors declare that this research was conducted in the absence of conflict of interest.


## AUTHOR CONTRIBUTIONS

BS collected and analysed the data, conducted the statistical analysis, prepared the figures and wrote the manuscript. HA recruited the patients and provided tumour samples. HAKB and EM collected the data. CH provided clinical data. ÅH and OTB organized the biobank and helped to provide clinical data. IØ provided supervision, discussed the results and contributed to the writing of the manuscript. AC designed and supervised the study, evaluated the experiments and wrote the manuscript. All authors have read and approved the final version of the manuscript.

## ORCID

Branislava Stankovic  <https://orcid.org/0000-0001-6355-8755>

[org/0000-0001-6355-8755](https://orcid.org/0000-0001-6355-8755)


Odd Terje Brustugun  <https://orcid.org/0000-0002-5153-8391>

[org/0000-0002-5153-8391](https://orcid.org/0000-0002-5153-8391)

Åslaug Helland  <https://orcid.org/0000-0002-5520-0275>

Inger Øynebråten  <https://orcid.org/0000-0001-8914-5676>

[org/0000-0001-8914-5676](https://orcid.org/0000-0001-8914-5676)

Alexandre Corthay  <https://orcid.org/0000-0001-9519-5725>

[org/0000-0001-9519-5725](https://orcid.org/0000-0001-9519-5725)

## REFERENCES

1. Travis WD. Pathology and diagnosis of neuroendocrine tumors: lung neuroendocrine. *Thorac Surg Clin.* 2014;24:257-266.
2. Travis WD, Brambilla E, Nicholson AG, et al. The 2015 World Health Organization Classification of Lung Tumors: impact of

- genetic, clinical and radiologic advances since the 2004 classification. *J Thorac Oncol.* 2015;10:1243-1260.
3. Rindi G, Klimstra David S, Abedi-Ardekani Behnoush, et al. A common classification framework for neuroendocrine neoplasms: an International Agency for Research on Cancer (IARC) and World Health Organization (WHO) expert consensus proposal. *Mod Pathol.* 2018;31(12):1770-1786.
  4. Naalsund A, Rostad H, Strom EH, Lund MB, Strand TE. Carcinoid lung tumors—incidence, treatment and outcomes: a population-based study. *Eur J Cardiothorac Surg.* 2011;39:565-569.
  5. Skuladottir H, Hirsch FR, Hansen HH, Olsen JH. Pulmonary neuroendocrine tumors: Incidence and prognosis of histological subtypes. A population-based study in Denmark. *Lung Cancer.* 2002;37(2):127-135.
  6. Fernandez-Cuesta L, Peifer M, Lu X, et al. Frequent mutations in chromatin-remodelling genes in pulmonary carcinoids. *Nat Commun.* 2014;5:3518.
  7. Vesterinen T, Mononen S, Salmenkivi K, et al. Clinicopathological indicators of survival among patients with pulmonary carcinoid tumor. *Acta Oncol.* 2018;57:1109-1116.
  8. Topalian SL, Hodi FS, Brahmer JR, et al. Safety, activity, and immune correlates of anti-PD-1 antibody in cancer. *N Engl J Med.* 2012;366:2443-2454.
  9. Gandhi L, Rodríguez-Abreu D, Gadgeel S, et al. Pembrolizumab plus chemotherapy in metastatic non-small-cell lung cancer. *N Engl J Med.* 2018;378:2078-2092.
  10. Hellmann MD, Ciuleanu T-E, Pluzanski A, et al. Nivolumab plus ipilimumab in lung cancer with a high tumor mutational burden. *N Engl J Med.* 2018;378:2093-2104.
  11. Lizotte PH, Ivanova EV, Awad MM, et al. Multiparametric profiling of non-small-cell lung cancers reveals distinct immunophenotypes. *JCI Insight.* 2016;1:e89014.
  12. Lavin Y, Kobayashi S, Leader A, et al. Innate immune landscape in early lung adenocarcinoma by paired single-cell analyses. *Cell.* 2017;169:750-765.e717.
  13. Stankovic B, Bjørhovde HAK, Skarshaug R, et al. Immune cell composition in human non-small cell lung cancer. *Front Immunol.* 2019;9:3101.
  14. Tsuruoka K, et al. PD-L1 expression in neuroendocrine tumors of the lung. *Lung Cancer.* 2017;108:115-120. <https://doi.org/10.1016/j.lungcan.2017.03.006>
  15. Kasajima A, Ishikawa Y, Iwata A, et al. Inflammation and PD-L1 expression in pulmonary neuroendocrine tumors. *Endocr Relat Cancer.* 2018;25:339-350.
  16. Wang H, Li Z, Dong B, et al. Prognostic significance of PD-L1 expression and CD8+ T cell infiltration in pulmonary neuroendocrine tumors. *Diagn Pathol.* 2018;13:30.
  17. Vesterinen T, Kuopio T, Ahtiainen M, et al. PD-1 and PD-L1 expression in pulmonary carcinoid tumors and their association to tumor spread. *Endocr Connect.* 2019;8:1168-1175.
  18. Katsenelson NS, Shurin GV, Bykovskaia SN, Shogan J, Shurin MR. Human small cell lung carcinoma and carcinoid tumor regulate dendritic cell maturation and function. *Mod Pathol.* 2001;14(1):40-45.
  19. Lardinois D, Deleyn P, Vanschil P, et al. ESTS guidelines for intra-operative lymph node staging in non-small cell lung cancer. *Eur J Cardiothorac Surg.* 2006;30:787-792.
  20. Kverneland AH, Streitz M, Geissler E, et al. Age and gender leucocytes variances and references values generated using the standardized ONE-Study protocol. *Cytometry A.* 2016;89:543-564.

## SUPPORTING INFORMATION

Additional supporting information may be found online in the Supporting Information section.

**How to cite this article:** Stankovic B, Aamodt H, Bjørhovde HAK, et al. The immune microenvironment in typical carcinoid lung tumor, a brief report of four cases. *Scand J Immunol.* 2020;92:e12893. <https://doi.org/10.1111/sji.12893>